

AD-A065 499

CHARLES STARK DRAPER LAB INC CAMBRIDGE MA

F/G 11/6

MATERIALS RESEARCH FOR ADVANCED INERTIAL INSTRUMENTATION. TASK --ETC(U)

FEB 79 J MCCARTHY, F PETRI

N00014-77-C-0388

UNCLASSIFIED

R-1231

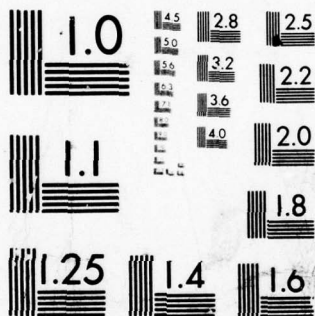
NL

| OF |  
AD  
A065 499



END  
DATE  
FILMED

4 --79  
DDC



MICROCOPY RESOLUTION TEST CHART  
NATIONAL BUREAU OF STANDARDS-1963-A

LEVEL

R-1231

AD A0 65499

DDC FILE COPY

**MATERIALS RESEARCH FOR ADVANCED  
INERTIAL INSTRUMENTATION**

**TASK 1: DIMENSIONAL STABILITY OF GYRO  
STRUCTURAL MATERIALS**

**TECHNICAL REPORT NO. 1  
FOR THE PERIOD  
1 OCTOBER 1977 - 30 SEPTEMBER 1978**

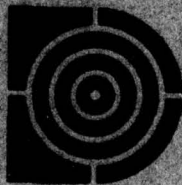
**BY**

**J. McCARTHY AND F. PETRI**

Prepared for the Office of Naval Research,  
Department of the Navy, under contract  
N0001-77-C-0388.

Approved for public release; distribution  
unlimited.

Permission is granted the U.S. Government  
to reproduce this paper in whole or in part.



**The Charles Stark Draper Laboratory, Inc.**  
Cambridge, Massachusetts 02139

79 03 05 073

REPORT DOCUMENTATION PAGE		READ INSTRUCTIONS BEFORE COMPLETING FORM
1. REPORT NUMBER TECHNICAL REPORT NO. 1	2. GOVT ACCESSION NO.	3. RECIPIENT'S CATALOG NUMBER
4. TITLE (and Subtitle) MATERIALS RESEARCH FOR ADVANCED INERTIAL INSTRUMENTATION TASK 1: DIMENSIONAL STABILITY OF GYRO STRUCTURAL MATERIALS		5. TYPE OF REPORT & PERIOD COVERED Research Report 10/1/77 - 9/30/78
7. AUTHOR(s) J. McCarthy and F. Petri		6. PERFORMING ORG. REPORT NUMBER R-1231
9. PERFORMING ORGANIZATION NAME AND ADDRESS The Charles Stark Draper Laboratory, Inc. 555 Technology Square, Cambridge, Massachusetts 02139 408 386		8. CONTRACT OR GRANT NUMBER(s) N00014-77-C-0388
11. CONTROLLING OFFICE NAME AND ADDRESS Office of Naval Research Department of the Navy 800 N. Quincy Street, Arlington, Virginia 22217		10. PROGRAM ELEMENT, PROJECT, TASK AREA & WORK UNIT NUMBERS
14. MONITORING AGENCY NAME & ADDRESS (if different from Controlling Office) Office of Naval Research - Boston Branch 666 Summer Street Boston, Massachusetts 02210 12 48 p.		12. REPORT DATE February 1979
		13. NUMBER OF PAGES 51
		15. SECURITY CLASS. (of this report) Unclassified
		15a. DECLASSIFICATION/DOWNGRADING SCHEDULE
16. DISTRIBUTION STATEMENT (of this Report)  Approved For Public Release, Distribution Unlimited.  Approved for public release, distribution unlimited.		
17. DISTRIBUTION STATEMENT (of the abstract entered in Block 20, if different from Report) 9 Technical rept. no. 1, 1 Oct 77 - 30 Sep 78		
18. SUPPLEMENTARY NOTES		
19. KEY WORDS (Continue on reverse side if necessary and identify by block number) Dimensional Stability      Microcreep Finite Element Analysis      Micromechanical Properties Gyroscope Materials      Microstrain Modeling Hot Isostatically Pressed Beryllium      Microyield Strength Instrument Materials		
20. ABSTRACT (Continue on reverse side if necessary and identify by block number) The literature is reviewed for micromechanical property data for materials used in precision instruments. Microyield strength and microcreep values are presented for general aluminum alloys, 440C stainless steel, and instrument grade beryllium. A method for applying finite element analysis techniques in conjunction with empirical data for instrument grade beryllium to predict micromechanical behavior of instrument components is discussed. A simple component configuration for experimental verification of the prediction technique is presented. The application of finite element techniques to the design of a composite microcreep specimen is presented. 408 386 (over) <i>over</i>		

79 03 05 073

The results of preliminary work on studies of micromechanical properties of hot isostatically pressed beryllium are presented. Test specimen preparation, microstrain instrumentation, and problems of alignment of loading are discussed.

ACCESSION for		on
NTIS		<input checked="" type="checkbox"/>
DDC		<input type="checkbox"/>
UNAWO		<input type="checkbox"/>
JUSTI		
BY		
DISTRIBUTION/AVAILABILITY CODES		SPECIAL
Dist.		
A		

R-1231

MATERIALS RESEARCH FOR ADVANCED  
INERTIAL INSTRUMENTATION

TASK 1: DIMENSIONAL STABILITY OF GYRO  
STRUCTURAL MATERIALS

TECHNICAL REPORT NO. 1  
FOR THE PERIOD

1 OCTOBER 1977 - 30 SEPTEMBER 1978

February 1979

By

J. McCarthy

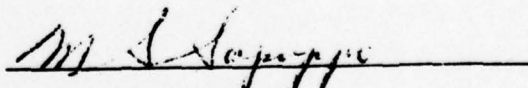
F. Petri

Prepared for the Office of Naval Research,  
Department of the Navy, under contract  
N00014-77-C-0388.

Approved for public release; distribution  
unlimited.

Permission is granted the U.S. Government  
to reproduce this paper in whole or in part.

APPROVED:



M. S. Sapuppo, Head  
Component Development Department

The Charles Stark Draper Laboratory, Inc.  
Cambridge, Massachusetts 02139

#### ACKNOWLEDGEMENTS

This report was prepared by The Charles Stark Draper Laboratory, Inc., under Contract N00014-77-C0388 with the Office of Naval Research of the Department of the Navy, with Dr. F. S. Gardner of ONR, Boston, serving as Scientific Officer.

Publication of this report does not constitute approval by the U.S. Navy of the findings or conclusions contained herein. It is published for the exchange and stimulation of ideas.

## TABLE OF CONTENTS

Section	Page
1. INTRODUCTION . . . . .	1
2. OBJECTIVES . . . . .	3
3. LITERATURE REVIEW. . . . .	5
4. MICROCREEP MODELING. . . . .	15
4.1 Objectives. . . . .	15
4.2 Analysis Of Test Specimens. . . . .	15
4.3 Selection Of Creep Laws . . . . .	16
5. THE MICROMECHANICAL BEHAVIOR OF HOT ISOSTATICALLY PRESSED BERYLLIUM. . . . .	25
5.1 General . . . . .	25
5.2 Work To Date. . . . .	26
5.3 Plans For Future Work . . . . .	35
References . . . . .	37

# LIST OF FIGURES

Figure		Page
1.	Axial stress plot, NBS test specimen. . . . .	16
2.	Axial stress plot, NBS test specimen. . . . .	17
3.	Magnified displacements, loaded NBS specimen. . . . .	18
4.	Strain versus time at room temperature. . . . .	20
5.	Strain versus time at 145°F . . . . .	21
6.	Proposed beryllium shrink fit cylinders . . . . .	24
7.	Transverse section of HIP50 billet 77014 showing orientation of specimen blanks. . . . .	27
8.	Typical HIP50 microstructure. . . . .	29
9.	Specimen for microyield and microcreep tests. . . . .	30
10.	Load train for microyield stress tests. . . . .	32
11.	Test setup for alignment tests. . . . .	34
12.	Typical load train for alignment tests . . . . .	35

# LIST OF TABLES

Table	Page
1. Aluminum alloy 2014-T6. . . . .	7
2. Aluminum alloy A356 . . . . .	8
3. Aluminum alloy 6061-T5. . . . .	9
4. Aluminum alloy 2024-T4. . . . .	10
5. Stainless steel 440C. . . . .	11
6. Stainless steel 440C. . . . .	12
7. Instrument grade beryllium. . . . .	13
8. Temperature dependence of microyield stress . . . . .	14
9. Properties of HIP50 Billet No. 77014. . . . .	28
10. Etching solution for HIP50 beryllium . . . . .	30

## SECTION 1

### INTRODUCTION

The knowledge of micromechanical behavior of materials is crucial to the design of accurate inertial guidance instruments. Earlier workers<sup>(1)</sup> have developed thermal treatments to minimize the effects of residual stresses and microstructural instabilities and have determined offset microyield stresses to be used in instrument design. However, the state of development of these very sensitive instruments is such that their overall accuracy can be improved by identifying the various sources of errors and mathematically modeling the effect with time and applying corrections. One such source of error is the microcreep which occurs in some of the stressed components of the instrument.

The following is the report of work done at The Charles Stark Draper Laboratory, Inc. (CSDL), from September 1977 to October 1978. The work is concurrent with a separate cooperative program at the National Bureau of Standards (NBS) with frequent communication of ideas and information.

NOT  
PRECEDING PAGE BLANK - FILMED

## SECTION 2 OBJECTIVES

The objectives of the CSDL effort are as follows:

- (1) Review the literature and summarize data on the microplastic behavior of materials used in inertial instruments.
- (2) Using finite element analysis methods and data from the literature, or measured by NBS or CSDL, model the micromechanical behavior of component parts of instruments. Verify the predicted behavior by test of a simple structural shape.
- (3) Investigate the micromechanical behavior of hot isostatically pressed beryllium as a more microcreep-resistant material for instruments.

In addition to the above major tasks, CSDL has assisted NBS by machining  $10^{-7}$  test specimens and by finite element stress analysis of proposed  $10^{-8}$  specimen designs. One of the objectives of the NBS program is to evaluate instrument-grade beryllium in a microstructural condition which is the same as the condition that exists in the instrument components. Therefore, the test specimens have been machined at CSDL using the same machining and stress relief techniques used for instrument manufacturers.

Preceding Page BLANK - NOT FILMED

### SECTION 3 LITERATURE REVIEW

The literature review has concentrated on hot isostatically pressed beryllium and on other metals used in instruments; NBS has surveyed the literature on hot pressed beryllium in their literature review<sup>(2)</sup>.

Microstrain measurement techniques have been used extensively for basic studies of microplasticity<sup>(3)</sup> and to a more limited extent for obtaining data for engineering materials. Marschall and Maringer<sup>(4)</sup> have extensively reviewed the topic of dimensional instability, including microplasticity, and provide a good bibliography through 1973.

Measurements of microcreep behavior provide the most valuable form of data for analysis of simple stress situations. Uniaxial tests most closely approximate actual stress conditions and are conducted in a way similar to macrocreep tests. The test specimen is incrementally loaded in the elastic range to establish an accurate value of modulus and then is loaded to the test stress in a constant load machine. The initial strain is measured as soon as possible after the full load is applied and measured periodically as a function of time. The instantaneous plastic strain is determined when the load is removed at the end of the test. The measurement of strain to a sensitivity of  $10^{-6}$  or smaller requires very tedious and expensive techniques; stability of instrumentation is extremely important. Maringer et al<sup>(5)</sup> and Marschall, Maringer, and Cepollina<sup>(6)</sup> have reported on tests conducted with foil gages. Marschall and Held<sup>(7)</sup> have described very elaborate methods for increasing the sensitivity of strain gage techniques.

Lyons<sup>(8)</sup> and Weihrauch and Horden<sup>(9)</sup> used capacitance gages to measure microcreep in various instrument materials. Polvani and Christ<sup>(10)</sup> recently reported results for elevated tests on instrument grade beryllium.

As an alternate to long-term microcreep tests, microyield tests have been used as a means of detecting the occurrence of the first measurable plastic strain. Although this test requires much less time and is more easily accomplished, it is much more dependent on test conditions such as sensitivity of measurement, strain rate, time at load, etc., and these variables must be carefully recorded when results are reported. However, when these facts are recognized and the value of microyield stress (MYS) is stated in terms of an offset of strain then MYS is a useful design guideline for selecting a maximum working stress. Instrumentation similar to that used for microcreep is used for microyield stress measurements. Maringer et al<sup>(5,11)</sup>, Imgram et al<sup>(12)</sup> and Marschall and Maringer<sup>(13)</sup> have reported values of microyield strength for a variety of instrument materials; these measurements were made with foil strain gages.

Microyield strength and microcreep data from all the above sources are summarized in Tables 1 through 7. The aluminum alloys are typical materials used for stable members of guidance systems, 440C stainless steel is the standard material for super-precision ball bearings, and beryllium is the basic structural material for inertial instruments. Table 8, from Weihrauch and Horden<sup>(9)</sup> shows the temperature dependence of microyield strength for typical materials.

It is obvious that there is a very limited amount of data regarding the microplastic behavior of engineering materials. For many alloys, there is considerable variance in the data that is available, in which case, the data can only be used as a qualitative guide. There is need for additional carefully controlled tests to more clearly define the microplastic behavior of instrument materials.

Table 1. Aluminum alloy 2014-T6<sup>(13)</sup>.

FORM: Sheet (Perpendicular to Rolling Direction).

CONDITION: T6 plus Stress Relief at 400°F for one hour.

STRAIN MEASUREMENT BY: Foil Strain Gages.

MICROYIELD STRESS (3 Specimens):

$\sigma_y$ (Microyield Stress) $\sim$ lb/in <sup>2</sup>			
Offset	$1 \times 10^{-6}$	$5 \times 10^{-6}$	$10 \times 10^{-6}$
	38,000	42,000	45,000

MICROCREEP (2 Specimens):

Strain at Time t ( $10^{-6}$ )			
Stress (lb/in <sup>2</sup> )	10 h	100 h	1,000 h
34,200	3	7	17

Table 2. Aluminum alloy A356<sup>(12)</sup>.

FORM: Cast

CONDITION: Solutionized at 1000°F for 16 hours, Boiling Water Quench

Aged at 310°F for 4 hours.

STRAIN MEASURED BY: Foil Strain Gages.

MICROYIELD STRESS (2 Specimens):

$\sigma_y$ (Microyield Stress) $\sim$ lb/in <sup>2</sup>				
Specimen No.	Offset	$1 \times 10^{-6}$	$5 \times 10^{-6}$	$10 \times 10^{-6}$
1		6,700	9,000	10,000
2		8,400	10,000	11,000

MICROCREEP (1 Specimen Each Stress):

Strain at Time t ( $10^{-6}$ )				
Stress (lb/in <sup>2</sup> )	1 h	10 h	100 h	1,000 h
4,000	0	1	8	17
6,000	0	0	0	10

Table 3. Aluminum alloy 6061-T6<sup>(6)</sup>.

FORM: Sheet (Parallel to Rolling Direction).

CONDITION: T6 plus Stress Relief for 1 hour at Temperature Shown.

STRAIN MEASURED BY: Foil Strain Gages.

MICROYIELD STRESS (2 Specimens Each Condition):

$\sigma_y$ (Microyield Stress) $\sim$ lb/in <sup>2</sup>				
Condition	Offset	$1 \times 10^{-6}$	$5 \times 10^{-6}$	$10 \times 10^{-6}$
T6		18,700	26,600	30,000
T6 + S.R. @ 400°F		26,300	30,800	32,800
T6 + S.R. @ 450°F		21,300	25,700	27,800
T6 + S.R. @ 500°F		13,700	18,100	20,600

MICROCREEP (1 Specimen Each Stress):

Condition: T6 + S.R. @ 400°F

Strain at Time t ( $10^{-6}$ )				
Stress (lb/in <sup>2</sup> )	1 h	10 h	100 h	1,000 h
14,800	-1	0	1	1
18,500	0	0	0	5
24,600	1	1	0	10

Table 4. Aluminum alloy 2024-T4<sup>(6)</sup>.

FORM: Sheet (Parallel to Rolling Direction)

CONDITION: T6 plus Stress Relief for 1 hour at Temperature Shown

STRAIN MEASUREMENT BY: Foil Strain Gages

MICROYIELD STRESS (2 Specimens Each Condition):

$\sigma_y$ (Microyield Stress) $\sim$ lb/in <sup>2</sup>				
Condition	Offset	$1 \times 10^{-6}$	$5 \times 10^{-6}$	$10 \times 10^{-6}$
T4		38,500	43,500	45,400
T4 + S.R. @ 400°F		32,300	40,800	45,000
T4 + S.R. @ 450°F		30,600	38,000	42,100
T4 + S.R. @ 500°F		21,400	29,100	32,900

MICROCREEP (1 Specimen Each Stress):

Condition: T4 +S.R. @ 400°F

Strain at Time t ( $10^{-6}$ )				
Stress (lb/in <sup>2</sup> )	1 h	10 h	100 h	1,000 h
18,000	0	0	1	5
24,000	0	0	2	7

Table 5. Stainless steel 440C<sup>(12)</sup>.

FORM: Bar

CONDITION: Austenitized at 1900°F for 30 minutes, Oil Quench

Subcool to -320°F for 30 minutes

Temper at 520°F for 1 hour

STRAIN MEASUREMENT BY: Foil Strain Gages

MICROYIELD STRESS (3 Specimens):

$\sigma_y$ (Microyield Stress) $\sim$ lb/in <sup>2</sup>			
Offset	$1 \times 10^{-6}$	$5 \times 10^{-6}$	$10 \times 10^{-6}$
	69,700	97,300	110,700

MICROCREEP (1 Specimen Each Stress):

Strain at Time t ( $10^{-6}$ )				
Stress (lb/in <sup>2</sup> )	1 h	10 h	100 h	1,000 h
33,500	0	0	0	0
50,000	0	0	2	6

Table 6. Stainless steel 440C<sup>(8)</sup>.

FORM: Bar

CONDITION: Austenitized at 1900°F for 30 minutes, Oil Quench.

Subcool to -100°F for 50 minutes.

Subcool to -320°F for 30 minutes.

Temper at 300°F for 2 hours.

Repeat Subcools.

Retemper at 300°F for 2 hours.

Stress Relieve at 300°F for 5 hours.

STRAIN MEASUREMENT BY: Capacitance Gage

MICROCREEP (1 Specimen):

Strain at Time t ( $10^{-6}$ )				
Stress (lb/in <sup>2</sup> )	1 h	10 h	100 h	1,000 h
82,000	-1	+1	0	+1

Table 7. Instrument grade beryllium<sup>(6)</sup>.

FORM: Hot Pressed Block.

CONDITION: As Indicated Below.

STRAIN MEASUREMENT BY: Foil Strain Gages.

MICROYIELD STRESS - CONDITION A (As Pressed)

$\sigma_y$ (Microyield Stress) in lb/in <sup>2</sup>			
Offset	$1 \times 10^{-6}$	$5 \times 10^{-6}$	$10 \times 10^{-6}$
Specimen 1	4,500	10,000	15,000
Specimen 2	7,000	14,000	20,000

MICROYIELD STRESS - CONDITION B (Stress Relieved at 1100°F for 1 hour)

$\sigma_y$ (Microyield Stress) in lb/in <sup>2</sup>			
Offset	$1 \times 10^{-6}$	$5 \times 10^{-6}$	$10 \times 10^{-6}$
Specimen 3	7,500	16,000	22,000
Specimen 4	9,000	16,000	22,000

MICROYIELD STRESS - CONDITION C (Stress Relieved at 1500°F for 1 hour)

$\sigma_y$ (Microyield Stress) in lb/in <sup>2</sup>			
Offset	$1 \times 10^{-6}$	$5 \times 10^{-6}$	$10 \times 10^{-6}$
Specimen 5	5,500	12,500	17,500
Specimen 6	10,000	17,500	23,000

MICROCREEP (1 Specimen Each Stress) (Stress Relieved at 1100°F for 1 hour)

Strain at Time t ( $10^{-6}$ )					
Stress (lb/in <sup>2</sup> )	1 h	10 h	100 h	1000 h	1400 h
4,500	0	1	2	8	9
5,600	0	1	1	4	5
7,000	0	1	1	6	7

Table 8. Temperature dependence of microyield stress <sup>(9)</sup> .

	MYS ( $5 \times 10^{-7}$ Offset) lb/in <sup>2</sup>		
	Temperature (°F)		
	75°	150°	200°
Aluminum 356-T6	8,100	7,350	7,190
Stainless Steel 310	22,700	20,400	20,000
Aluminum 6061-T6	12,400	11,700	10,430
Magnesium AZ92A	5,280	5,040	4,780

STRAIN MEASURED BY: Capacitance Gage

## SECTION 4

### MICROCREEP MODELING

#### 4.1 OBJECTIVES

The analytical program in support of the NBS Test Program is designed to apply data from uniaxial test specimens to actual three-dimensional gyro structure parts. Existing analytical methods for macrocreep will be used to predict growth due to microcreep of typical structures. Work accomplished in fiscal year 1978 included:

- (1) Analysis of the stress distribution in typical NBS test specimens.
- (2) Selection of creep laws for preliminary analysis.
- (3) Selection of possible design components for analysis and test.

#### 4.2 ANALYSIS OF TEST SPECIMENS

One of the proposed specimens for the NBS  $10^{-8}$  microcreep tests is a dumb-bell shaped specimen. Eight node quadratic axisymmetric elements were selected in the MARC Analysis Program to analyze stress concentrations in the specimen. The model consisted of 16 elements and 65 nodes. A plot of the mesh is shown in Figure 1. Elements 15 and 16 were loaded with a uniform pressure loading so as to produce a uniform tensile stress of 15,000 lb/in<sup>2</sup> in the test length of the specimen. The resulting axial stress distribution is shown in Figure 2.

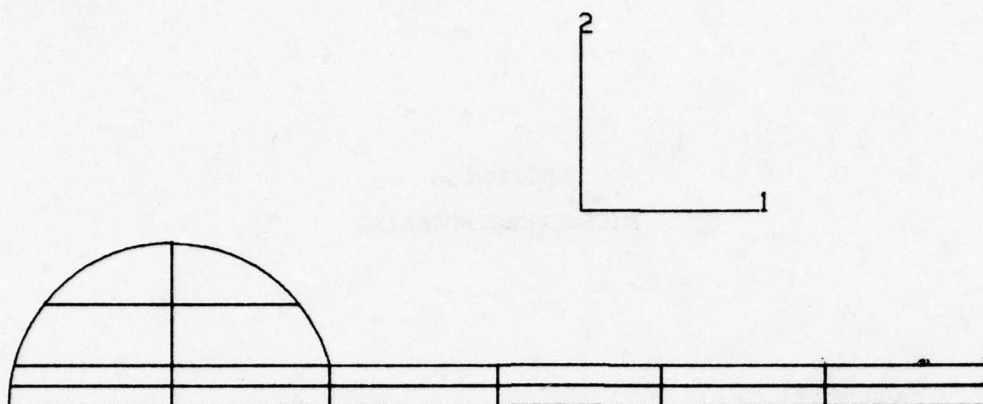


Figure 1. Axial stress plot, NBS test specimen.

As may be seen, about 90 percent of the 1/4 inch rod is at the uniform stress of  $1\text{b/in}^2$ . The 10-percent region near the spherical ball starts a sharp transition to a low stress region. The majority of the spherical ball is in a low stress state. There exists no stress concentration region for this shape. A highly magnified display of the displacements, due to this load, is shown in Figure 3. The spherical ball is deformed into a teardrop shape as a result of the loading.

#### 4.3 SELECTION OF CREEP LAWS

##### 4.3.1 Uniaxial Microcreep Law

In order to select a creep law for instrument-grade beryllium, the results of previous investigators were reviewed<sup>(6,8,10,12)</sup>. Reference 10 reports the initial work of Christ and Polvani at NBS. Although the authors report different creep rates at similar stress levels, almost all data indicates an essentially linear growth with time for the first 1000 hours. This is a different phenomena than generally observed at the macrocreep level where an exponential behavior with time is typical. Prior to this work, most measurements were made at room temperature; the NBS work was performed at  $144^\circ\text{F}$ . A creep law of the form:

- 1 = -304 E3
- 2 = .786 E3
- 3 = .187 E4
- 4 = 296 E4
- 5 = .406 E4
- 6 = 515 E4
- 7 = 624 E4
- 8 = 733 E4
- 9 = 842 E4
- 10 = 951 E4
- 11 = .106 E5
- 12 = .117 E5
- 13 = .127 E5
- 14 = .138 E5
- 15 = .149 E5

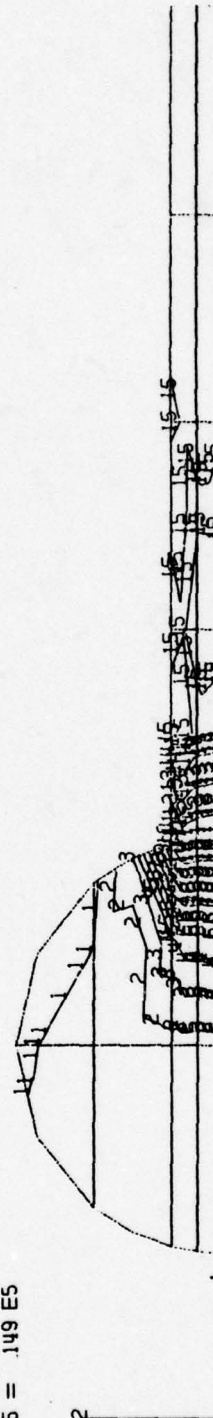


Figure 2. Axial stress plot, NBS test specimen.

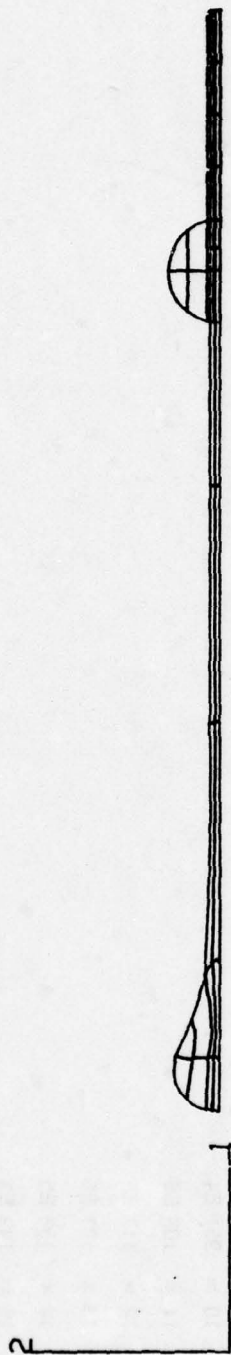


Figure 3. Magnified displacements, loaded NBS specimen.

$$\Sigma = A \sigma^n e^{-\frac{\Delta H}{RT}} t$$

is assumed where:

$\Sigma$  = total strain

A = a constant

$\sigma$  = uniaxial stress

n = stress exponent

$\Delta H/R$  = activation constant

T = absolute temperature

t = time

Much of the observed data can be fitted with the following constants:

A = 123

n = 0.25

$\Delta H/R$  = 6500

The units assumed for these constants are:

$\Sigma$  = microinches/inches

$\sigma$  = lb/in<sup>2</sup>

T = °R

t = hours

Plots at stresses of 2000, 4000, 6000, 8000 and 10,000 lb/in<sup>2</sup> at room temperature and 144°F are shown in Figures 4 and 5. Also shown are some of the measured data points. This fit is meant to be only a first approximation of available data, in order to proceed with the modeling of three-dimensional shapes. As more data becomes available, the constants will be updated.

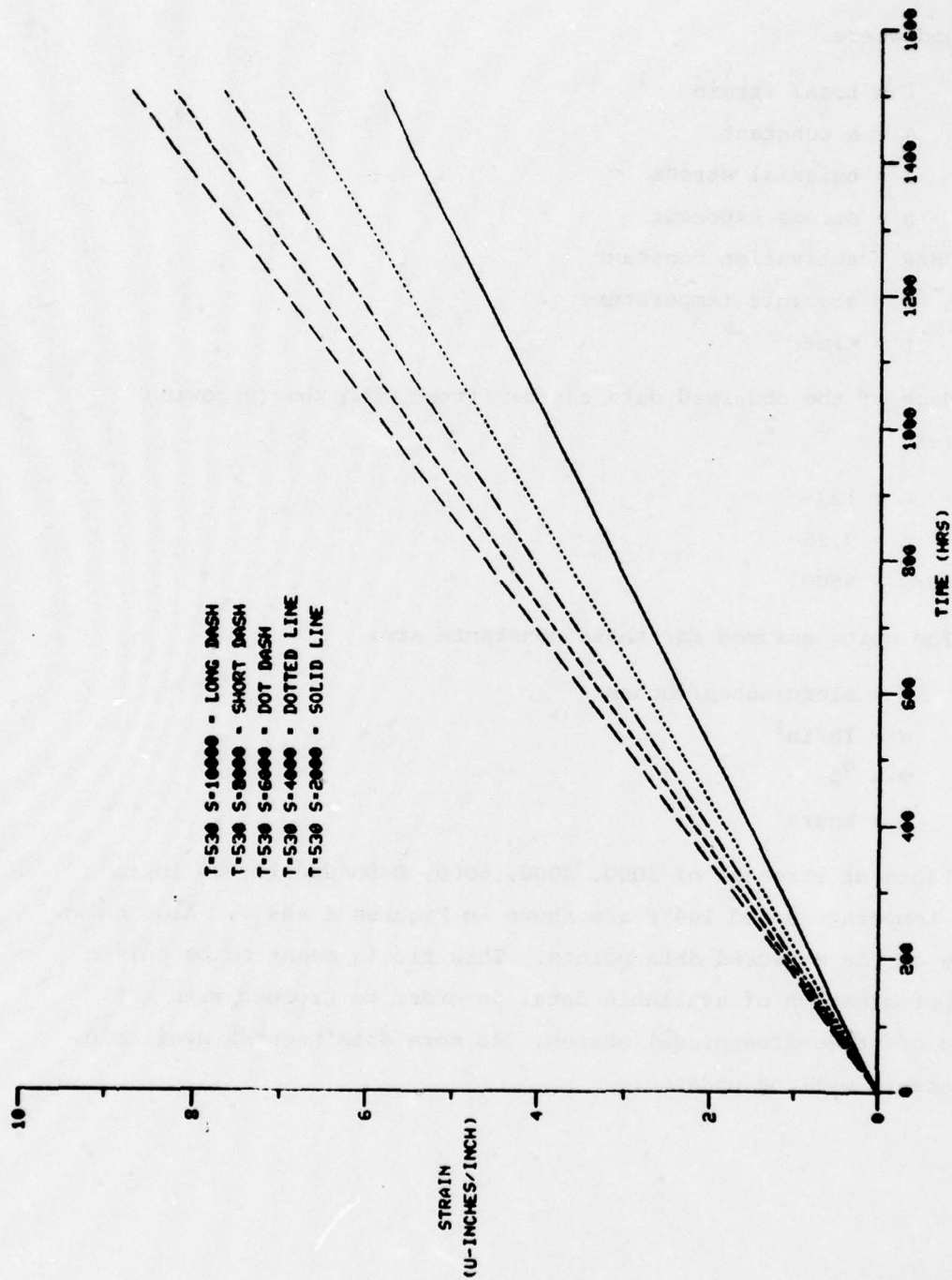


Figure 4. Strain versus time at room temperature.

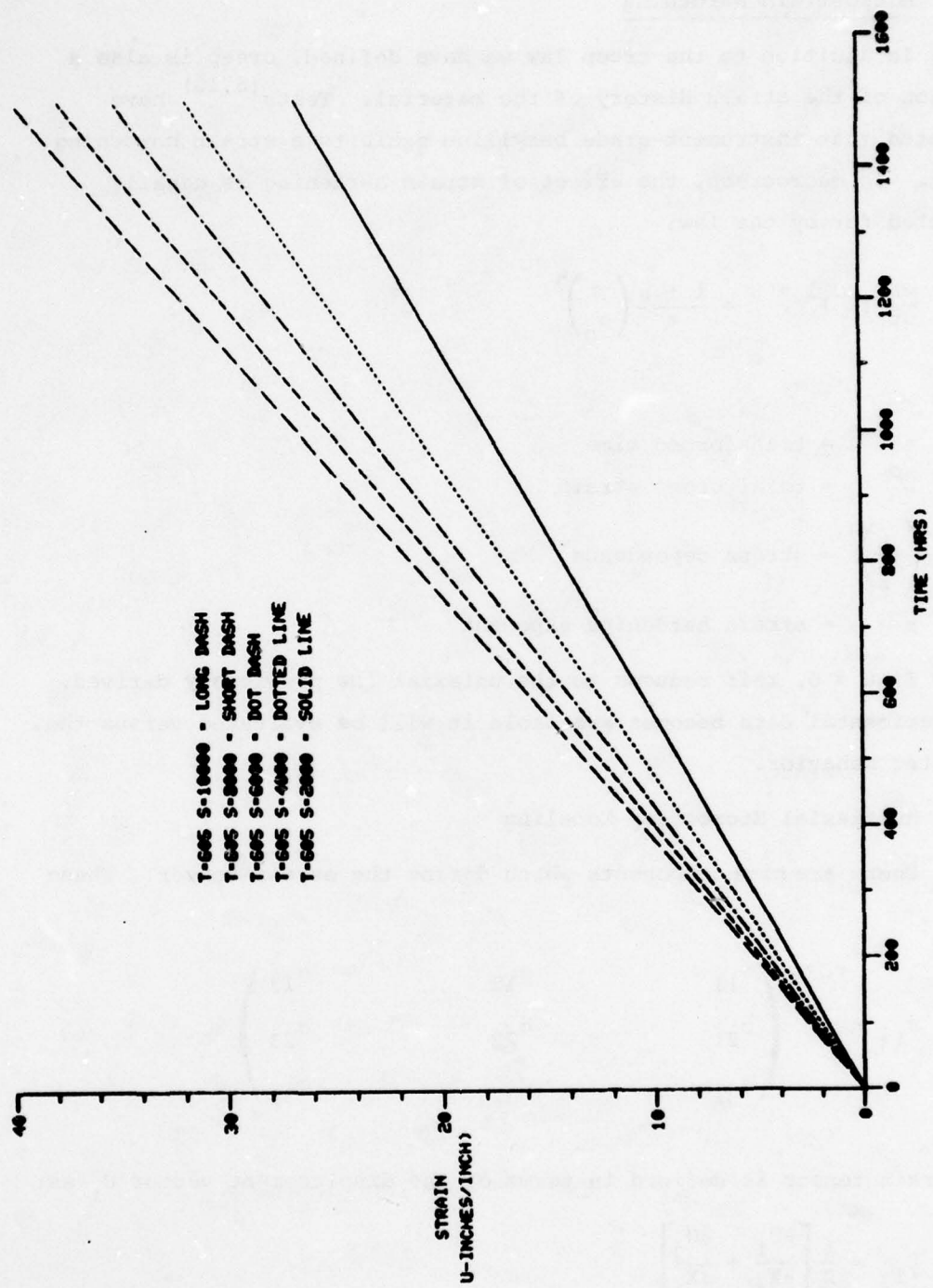


Figure 5. Strain versus time at 145°F.

#### 4.3.2 Microstrain Hardening

In addition to the creep law we have defined, creep is also a function of the strain history of the material. Tests<sup>(6,10)</sup> have indicated that instrument-grade beryllium exhibits a strain hardening effect. In macrocreep, the effect of strain hardening is usually accounted for by the law:

$$\frac{d}{dt} [\Sigma^C]^{1+\mu} = \frac{1+\mu}{\tau} \left( \frac{\sigma}{\sigma_n} \right)^n$$

where:

$\tau$  = transformed time  
 $\Sigma^C$  = total creep strain

$\left( \frac{\sigma}{\sigma_n} \right)^n$  = stress dependence

$\mu$  = strain hardening exponent

If  $\mu = 0$ , this reduces to the uniaxial law previously derived. As experimental data becomes available it will be evaluated versus the predicted behavior.

#### 4.3.3 Multiaxial Microcreep Modeling

There are nine components which define the stress tensor. These are:

$$\sigma_{ij} = \begin{pmatrix} \sigma_{11} & \sigma_{12} & \sigma_{13} \\ \sigma_{21} & \sigma_{22} & \sigma_{23} \\ \sigma_{31} & \sigma_{32} & \sigma_{33} \end{pmatrix}$$

The strain tensor is defined in terms of the displacement vector  $U_i$  as:

$$\Sigma_{ij} = \frac{1}{2} \left[ \frac{\partial U_i}{\partial X_j} + \frac{\partial U_j}{\partial X_i} \right]$$

In order to apply the uniaxial creep law defined previously, an effective stress  $\sigma_e$  is defined by:

$$\sigma_e^2 = 3/2 S_{ij} S_{ij}$$

where  $S_{ij}$  is the stress deviator and is defined by:

$$S_{ij} = \sigma_{ij} - 1/3 \sigma_{kk} \delta_{ij}$$

where  $\delta_{ij}$  is the unit tensor defined by:

$$\delta_{ij} = \begin{cases} 1 & \text{when } i = j \\ 0 & \text{when } i \neq j \end{cases}$$

This definition of an effective stress satisfies the following conditions:

- (1) For a condition of uniaxial stress, the multiaxial equations degenerate to the uniaxial condition.
- (2) The equations allow for the volume constancy of creep deformation.
- (3) A superimposed hypostatic state of stress will not result in a change of creep rate.
- (4) For an isotropic medium, the principal directions of strain and stress coincide.

#### 4.4 SELECTION OF STRUCTURAL COMPONENT FOR ANALYSIS

In order to verify that the uniaxial creep law can be applied to a three-dimensional component, a test of a relatively simple component is proposed.

The wheel is a critical component of a gyro, which is usually stressed at levels which are a significant percentage of the microyield stress. These stresses are caused by both the shrink fit forces of an outer rim on an inner hub, and centrifugal spin forces. A simple test would consist of two shrink fit beryllium cylinders controlled at 145°F. A picture of the proposed configuration is shown in Figure 6.

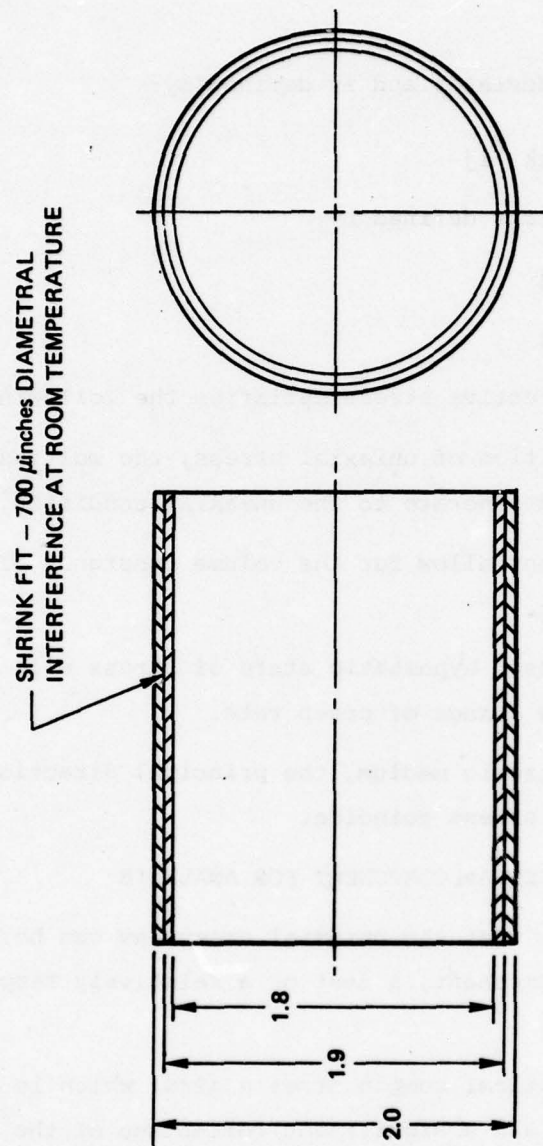


Figure 6. Proposed beryllium shrink fit cylinders.

SECTION 5  
THE MICROMECHANICAL BEHAVIOR OF  
HOT ISOSTATICALLY PRESSED BERYLLIUM

5.1 GENERAL

Beryllium has been an important structural material in inertial gyroscopes and related instruments for nearly twenty years. Although beryllium has very significant advantages in terms of high elastic modulus, low density, and good thermal conductivity, the high oxide grades currently used for highly stressed components have low ductility, only moderate resistance to microplastic deformation, and, in gas bearing use, provide a very inhomogeneous surface for thin coatings. Recent investigations have indicated that moderate purity beryllium which is consolidated by hot isostatic pressing may offer substantial improvements in the above areas.

Sheminski and Maringer<sup>(14)</sup> investigated the microstrain characteristics of several compositions of beryllium which were fabricated by hot isostatic pressing and found that microyield strength increased with decreasing grain size when the specimen was heat treated after pressing. They also found that MYS increased with decreasing pressing temperature. Gelles<sup>(15)</sup> has summarized the impurity reactions which have been found to occur in beryllium and their effect on mechanical properties. Foos et al<sup>(16)</sup> have proposed that the primary microalloying reaction in beryllium is between iron, aluminum, and beryllium and that microyield strength is increased by maximizing the dispersion of  $\text{FeBe}_{11}$ . London et al<sup>(17)</sup> have studied the effect of grain size in hot isostatically pressed, high purity powders and have concluded that grain size is the

most important single variable influencing yield strength and suggest that microyield strength is similarly affected. Keith<sup>(18)</sup> has found that the MYS of commercially produced hot isostatically pressed beryllium can be significantly influenced by aging heat treatments.

The objective of the present investigation is to study the microplastic deformation characteristics of HIP50 beryllium and the mechanisms that control it.

## 5.2 WORK TO DATE

### 5.2.1 Material

The hot isostatically pressed beryllium was supplied by Kawecki Berylco Industries (KBI) in the form of specimen blanks 0.7 inch square by 3 inches long. The blanks were cut from the bottom of billet 77014 which was 7.25 inches diameter by 15.5 inches high. The billet was hot isostatically pressed at 1950°F from impact-attributed powder. The time-temperature schedule consisted of three hours heating to pressing temperature, press at 15,000 lb/in<sup>2</sup> for five hours, and cool to 300°F in three hours. Isostatic pressure was reduced during cooling. All blanks were oriented transversely to the pressing direction; Figure 7 shows their relative location. The beryllium was supplied as KBI grade HIP50; the properties reported by the manufacturer are given in Table 9. Typical microstructure is shown in Figure 8.

### 5.2.2 Test Specimen Preparation

The same cylindrical-design test specimen is used for both the MYS tests and microcreep tests. The specimen is shown in Figure 9. The specimens are machined on centers with close attention to tolerances to attain optimum uniformity of applied stress. Machining methods are similar to those described in Materials Advisory Board report MAB-205-M<sup>(19)</sup>. Heat treatment is performed before machining the final 0.010 inch of material from the gage section. Although a recent study<sup>(20)</sup> shows that the above method leaves no significant surface damage when evaluated by macromechanical property tests the gage section of the specimens is etched to remove any possible surface damage.

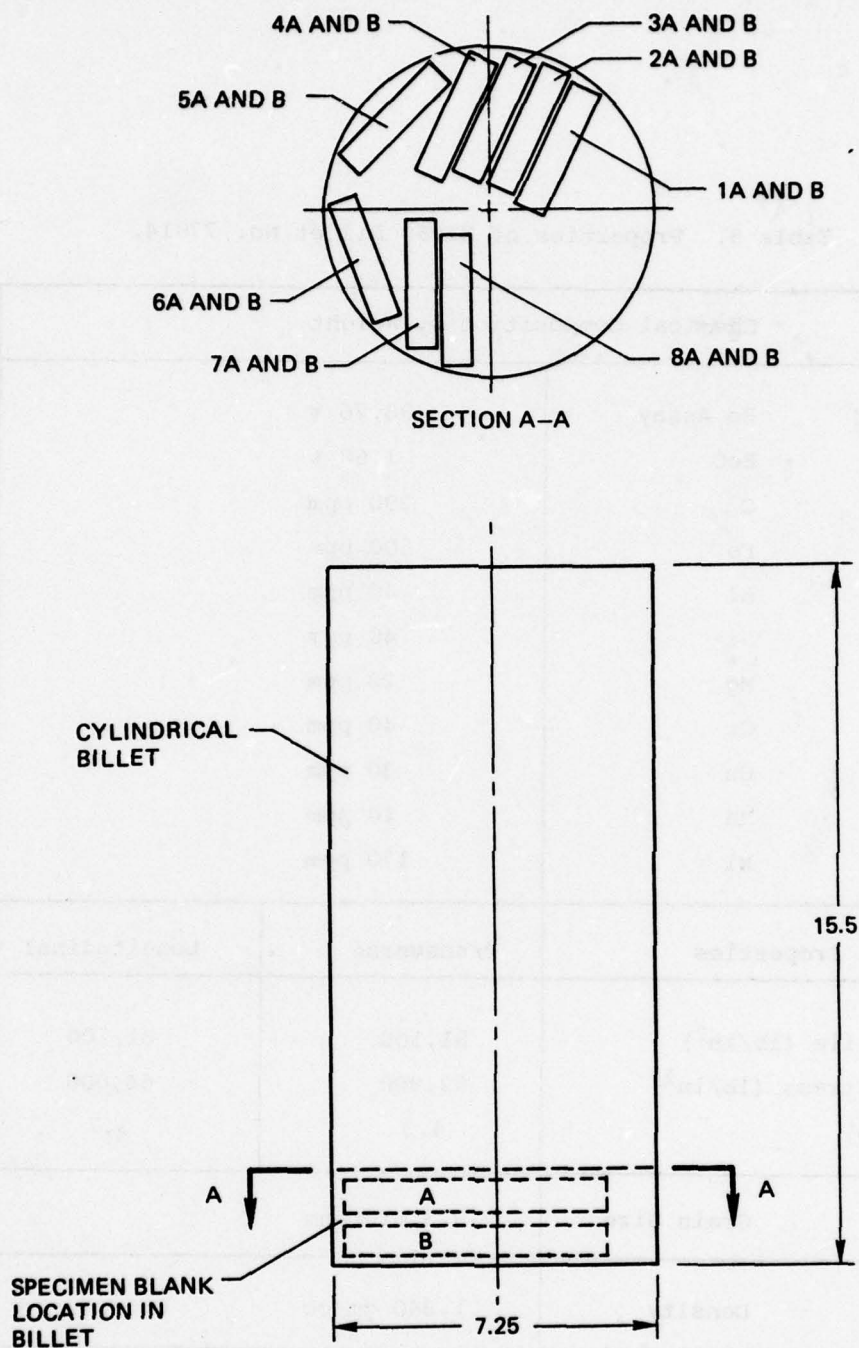


Figure 7. Transverse section of HIP50 billet 77014 showing orientation of specimen blanks.

Table 9. Properties of HIP50 Billet No. 77014.

Chemical Composition by Weight		
Be Assay	98.76 %	
BeO	1.68 %	
C	290 ppm	
Fe	500 ppm	
Al	40 ppm	
Si	40 ppm	
Mg	20 ppm	
Cr	40 ppm	
Cu	30 ppm	
Mn	10 ppm	
Ni	170 ppm	
Mechanical Properties	Transverse	Longitudinal
Ultimate Tensile (lb/in <sup>2</sup> )	81,100	81,100
0.2 % Yield Stress (lb/in <sup>2</sup> )	62,900	64,000
Elongation (%)	4.3	3.7
Grain Size	9.3 microns	
Density	1.840 gm/cc	



Figure 8. Typical HIP50 microstructure.

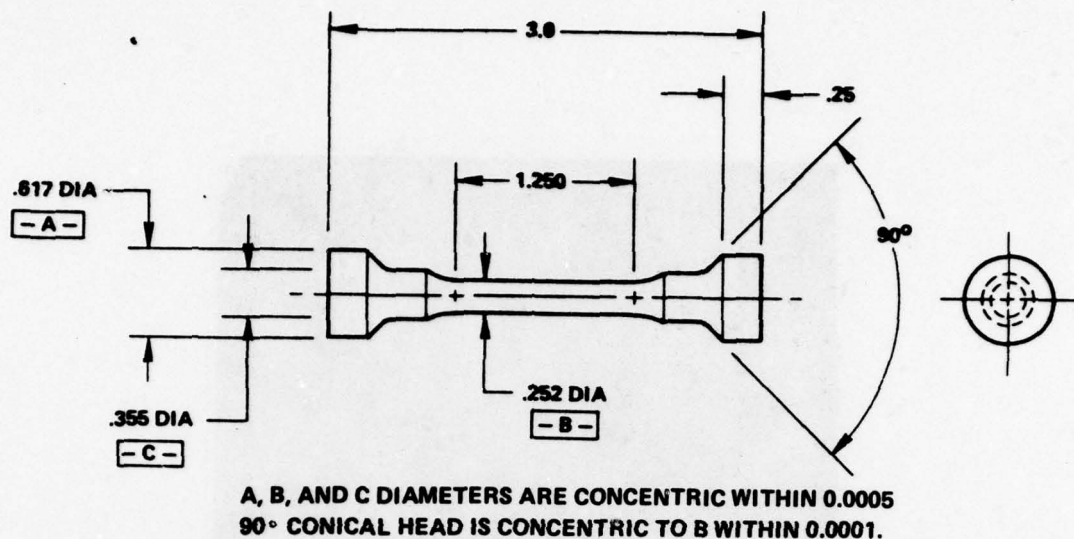


Figure 9. Specimen for microyield and microcreep tests.

The ends of the test specimen are masked by brushing on "Microflex" stop-off<sup>\*</sup>; the stop-off is dried and the gage section etched until 0.006 inch of material is removed from the diameter. The composition of the etching solution is given in Table 10. The specimen is removed periodically, rinsed in warm water, followed by cold water, dried with alcohol, and measured. The stop-off is subsequently dissolved in acetone.

Table 10. Etching solution for HIP50 beryllium.

50 ml $H_2SO_4$
50 ml $H_3PO_4$
300 ml $H_2O$
75 gm $CrO_3$

Bath temperature should be controlled between 49° to 54°C and stirred vigorously.

<sup>\*</sup> Manufactured by Michigan Chrome and Chemical Co., Detroit, Michigan.

### 5.2.3 Strain Gage Installation

Foil strain gages, Micro-Measurements type MA-06-125AD-120, are used to measure microstrain during MYS tests. Three gages with axes equally spaced around the circumference of the gage diameter are bonded to the specimen with M-Bond 600 epoxy adhesive. Application details are given in Bulletin B-130-6<sup>(22)</sup>. By means of the three gages, it is possible to measure the precision of alignment of the specimen during test. The specimen surface is not abraded but treated with metal conditioner followed by neutralizer. Each gage is carefully aligned axially, bonded, and cured individually. Gages are clamped with special formed pads which apply a uniform 40 to 50 lb/in<sup>2</sup> pressure during curing. The adhesive is cured at 250°F for two hours followed by a postcure, without clamps, at 300°F for an additional two hours. After bonding each gage, the area along the sides of each gage is cleaned of excess cement before bonding the adjoining gage. Lead wires are then soldered to each gage through a stress-relief solder tab and the gages and lead wires coated with microcrystalline wax to exclude moisture.

### 5.2.4 Alignment of Loading

The axial alignment of load in MYS tests is particularly critical in order to assure uniform stress conditions in the specimen gage length. Without uniform stress conditions indicated plastic strain may be the result of localized bending stresses rather than general plastic deformation. The load train which is used for these experiments is shown in Figure 10. The train depends on accurate control of geometry in the specimen, split plates, and specimen holder combined with flexible rod end bearings to achieve alignment of loading. The conical head of the test specimen centers itself into the fitted seat of the split plates which in turn are a close-slide-fit in the U-opening in the specimen holder.

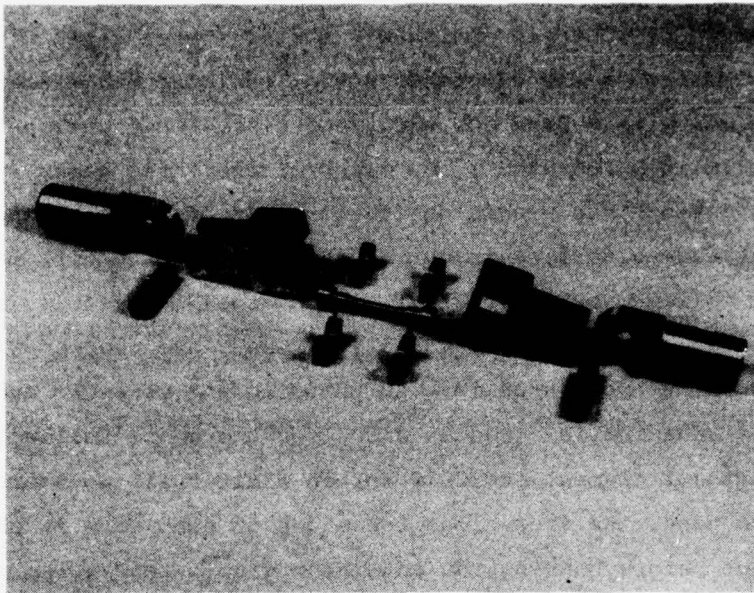


Figure 10. Load train for microyield stress tests.

A method for determining maximum surface strain on a cylindrical specimen from the readings of three strain gages located 120 degrees apart around the diameter has been developed by Morrison<sup>(23)</sup>. Christ and Swanson<sup>(24)</sup> have adapted this formula to define a precision of alignment (P) which provides a measure of extreme surface bending strain independent of total strain. Precision of alignment is defined as:

$$P = \frac{2 \Sigma_b \ell_o}{d}$$

where:

$\ell_o$  = specimen gage length

$d$  = specimen diameter

and  $\Sigma_b$  is related to the three strain readings by:

$$\Sigma_b = \frac{2}{3} \sqrt{(\Delta\Sigma_A)^2 + (\Delta\Sigma_B)^2 - \Delta\Sigma_A \Delta\Sigma_B}$$

$$\Delta\Sigma_A = (\Sigma_1 - \Sigma_3)$$

$$\Delta\Sigma_B = (\Sigma_2 - \Sigma_3)$$

and  $\Sigma_1$ ,  $\Sigma_2$ , and  $\Sigma_3$  are the three strain gage readings in decreasing magnitude.

In order to determine the degree of misalignment in the load train to be used for the MYS and microcreep tests, a test specimen was made from AISI 416 stainless steel and instrumented with three strain gages in the same way as a MYS sample. The specimen was placed in the load train in an Instron testing machine and loaded to 5000 lb/in<sup>2</sup> which is a typical low stress for MYS tests. The three strain gages were connected to a BLH Type N strain indicator through a switch box and were individually read to determine precision of alignment (P). The test arrangement is shown in Figures 11 and 12. Precision of alignment varied between  $3 \times 10^{-5}$  and  $5 \times 10^{-4}$ . The split plates are now being reworked to attain more uniform contact with the specimen. A consistent value of  $P = 5 \times 10^{-5}$  will give an extreme surface bending stress of 250 lb/in<sup>2</sup> which is a reasonable value for our tests.

### 5.3 Plans for Future Work

During the next fiscal year microyield tests will be conducted on HIP50 in the as-pressed condition and after various thermal treatments. Thermal treatments would be chosen so as to both achieve thermal stress relief of machining stresses and to increase the MYS by precipitation reactions. Metallographic studies will be performed on material before and after MYS tests. Microcreep studies will also be performed on these materials.



Figure 11. Test setup for alignment tests.

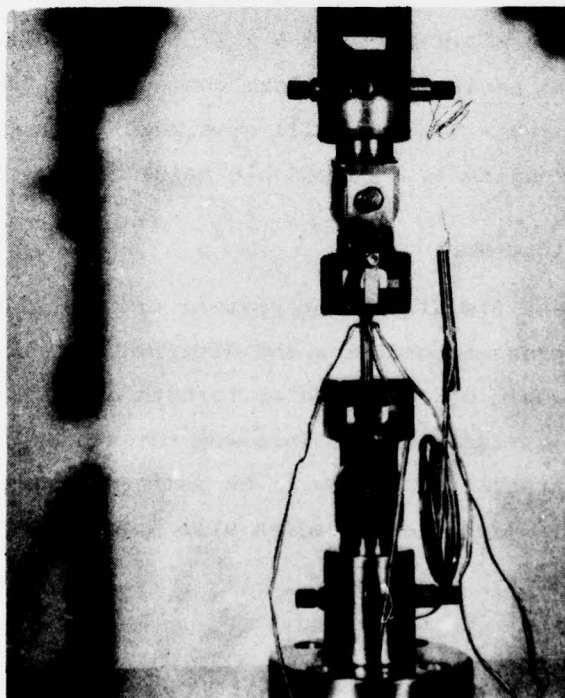


Figure 12. Typical load train for alignment tests.

#### REFERENCES

1. Lement, B. S., and B. L. Averbach, Measurement and Control of the Dimensional Behavior of Metals, Report R-95, Massachusetts Institute of Technology, December 1955.
2. Christ, B. W., and R. S. Polvani, A Review of the Micromechanical Properties of Various Grades of Beryllium, NBS Report (in preparation).
3. McMahon, Jr., C. J., Editor, Microplasticity, Wiley, New York, 1968.
4. Marschall, C. W., and R. E. Maringer, Dimensional Instability, An Introduction, Pergamon Press, Oxford, 1977.
5. Maringer, R. E., M. M. Chu, A. G. Imgram, and F. C. Holden, Stability of Structural Materials for Spacecraft Application, First Topical Report on Contract NAS5-10267, Battelle Memorial Institute, Columbus, Ohio, 1967.
6. Marschall, C. W., R. E. Maringer, and F. J. Cepollina, AIAA Paper No. 72-325, 13th Structures, Structural, Dynamics, and Materials Conference, 1972.
7. Marschall, C. W., and P. R. Held, Strain, January 1977.
8. Lyons, Jr., J. W., Absolute Capacitance Microcreep and Dimensional Stability Measuring System, Report NASA TMX-2046, Washington, DC, 1971.

9. Weihrauch, P. F., and M. J. Hordon, The Dimensional Stability of Selected Alloy Systems, Final Report Under Contract N140(131) 75098B, Alloyd General Corp., Cambridge, MA, 1964.
10. Christ, B. W., and R. S. Polvani, Micromechanical Properties of Instrument Grade Beryllium, NBS Report (in preparation).
11. Maringer, R. E., M. M. Cho, A. G. Imgram, and F. C. Holden, Stability of Structural Materials for Spacecraft Application, Second Topical Report on Contract NAS5-10267, Battelle Memorial Institute, Columbus, Ohio, 1967.
12. Imgram, A. G., M. E. Hoskins, J. H. Sovik, R. E. Maringer, and F. C. Holden, Study of Microplastic Properties and Dimensional Stability of Materials, Technical Report AFML-TR-67-232, Part II, Battelle Memorial Institute, Columbus, Ohio, 1968.
13. Marschall, C. W., and R. E. Maringer, Journal of Materials, Vol. 6, No. 2, 1971, p. 374-387.
14. Sheminski, R. M., and R. E. Maringer, Journal of the Less-Common Metals, Vol. 17, 1969, p. 25-45.
15. Gelles, S. H., Impurity Effects in Beryllium, Report MCIC-72-06, Metals and Ceramics Information Centers, Battelle Columbus Laboratories, Columbus, Ohio, 1972.
16. Foos, R. A., A. J. Stonehouse, and K. A. Walsh, Micro-Alloying Relationships in Beryllium, Report BBC-TR-456, The Brush Beryllium Co., Cleveland, Ohio, 1970.
17. London, G. J. G. H. Keith, and N. P. Pinto, Metals Engineering Quarterly, November 1976, p. 45-57.
18. Keith, G. H., Kawecky Berylco Industries, Unpublished Communication, September 1978.
19. Materials Advisory Board, Evaluation Test Methods for Beryllium, Report MAB-205-M, National Academy of Sciences, National Research Council, Washington, DC, 1966.

20. Hanafee, J. E., Effect of Machining on Properties of Impact-Ground Beryllium, Report UCRL-52287, Lawrence Livermore Laboratory, Livermore, CA, 1977.
21. Keith, G. H., Kawecki Berylco Industries, Private Communication, 1978.
22. Micro-Measurements, Strain Gage Installations with M-Bond 43-B, 600, and 610 Adhesives, Instruction Bulletin B-130-6, Vishay Intertechnology, Inc., Romulus, Michigan, 1977.
23. Morrison, J. L. M., Proceedings of the Institute of Mechanical Engineers, Vol. 142, No. 1, 1939, p. 220.
24. Christ, B. W., and S. R. Swanson, Journal of Testing and Evaluation, Vol 4, No. 6, 1976, p. 405-417.

BASIC DISTRIBUTION LIST

ORGANIZATION	COPIES	ORGANIZATION	COPIES
Defense Documentation Center Cameron Station Alexandria, VA 22314	12	Naval Air Propulsion Test Center Trenton, NJ 08628 ATTN: Library	1
Office of Naval Research Department of the Navy 800 N. Quincy Street Arlington, VA 22217	1	Naval Construction Battalion Civil Engineering Laboratory Port Hueneme, CA 93043 ATTN: Materials Division	1
ATTN: Code 471	1	Naval Electronics Laboratory San Diego, CA 92152	
Code 102	1	ATTN: Electron Materials Sciences Division	1
Code 470	1		
Commanding Officer Office of Naval Research Branch Office Building 114, Section D 666 Summer Street Boston, MA 02210	1	Naval Missile Center Materials Consultant Code 3312-1 Point Mugu, CA 92041	1
Commanding Officer Office of Naval Research Branch Office 536 South Clark Street Chicago, IL 60605	1	Commanding Officer Naval Surface Weapons Center White Oak Laboratory Silver Spring, MD 20910 ATTN: Library	1
Office of Naval Research San Francisco Area Office 760 Market Street, Room 447 San Francisco, CA 94102	1	David W. Taylor Naval Ship Research and Development Center Materials Department Annapolis, MD 21402	1
Naval Research Laboratory Washington, DC 20375		Naval Undersea Center San Diego, CA 92132 ATTN: Library	1
ATTN: Code 6000	1	Naval Underwater System Center Newport, RI 02840	
Code 6100	1	ATTN: Library	1
Code 6300	1		
Code 6400	1	Naval Weapons Center China Lake, CA 93555	
Code 2627	1	ATTN: Library	1
Naval Air Development Center Code 302 Warminster, PA 18964 ATTN: Mr. F. S. Williams	1	Naval Postgraduate School Monterey, CA 93940 ATTN: Mechanical Engineering Department	1

# BASIC DISTRIBUTION LIST (continued)

ORGANIZATION	COPIES	ORGANIZATION	COPIES
Naval Air Systems Command Washington, DC 20360 ATTN: Code 52031 Code 52032	1 1	NASA Headquarters Washington, DC 20546 ATTN: Code RRM	1
Naval Sea System Command Washington, DC 20362 ATTN: Code 035	1	NASA (216) 433-4000 Lewis Research Center 21000 Brookpark Road Cleveland, OH 44135 ATTN: Library	1
Naval Facilities Engineering Command Alexandria, VA 22331 ATTN: Code 03	1	National Bureau of Standards Washington, DC 20234 ATTN: Metallurgy Division Inorganic Materials Division	1
Scientific Advisor Commandant of the Marine Corps Washington, DC 20380 ATTN: Code AX	1	Director Applied Physics Laboratory University of Washington 1013 Northeast Fortieth Street Seattle, WA 98105	1
Naval Ship Engineering Center Department of the Navy Washington, DC 20360 ATTN: Code 6101	1	Defense Metals and Ceramics Information Center Battelle Memorial Institute 505 King Avenue Columbus, OH 43201	1
Army Research Office P.O. Box 12211 Triangle Park, NC 27709 ATTN: Metallurgy and Ceramics Program	1	Metals and Ceramics Division Oak Ridge National Laboratory P.O. Box X Oak Ridge, TN 37380	1
Army Materials and Mechanics Research Center Watertown, MA 02172 ATTN: Research Programs Office	1	Los Alamos Scientific Laboratory P.O. Box 1663 Los Alamos, NM 87544 ATTN: Report Librarian	1
Air Force Office of Scientific Research Bldg. 410 Bolling Air Force Base Washington, DC 20332 ATTN: Chemical Science Directorate Electronics and Solid State Sciences Directorate	1	Argonne National Laboratory Metallurgy Division P.O. Box 229 Lemont, IL 60439	1

# BASIC DISTRIBUTION LIST (continued)

ORGANIZATION	COPIES	ORGANIZATION	COPIES
Air Force Materials Laboratory Wright-Patterson AFB Dayton, OH 45433	1	Brookhaven National Laboratory Technical Information Division Upton, Long Island New York 11973	
Library Building 50, Rm 134 Lawrence Radiation Laboratory Berkeley, CA	1	ATTN: Research Library	1
		Office of Naval Research Branch Office 1030 East Green Street Pasadena, CA 91106	1

SUPPLEMENTARY DISTRIBUTION LIST

Dr. Bruce W. Christ  
National Measurement Laboratory  
National Bureau of Standards  
Washington, DC 20234

Dr. R. S. Polvani  
National Measurement Laboratory  
National Bureau of Standards  
Washington, DC 20234

Dr. A. W. Ruff, Jr.  
National Measurement Laboratory  
National Bureau of Standards  
Washington, DC 20234

Dr. Robert Hocken  
National Engineering Laboratory  
National Bureau of Standards  
Washington, DC 20234

Dr. Gilbert J. London  
Code 6063  
Naval Air Development Center  
Warminster, PA 18974

Professor G. S. Ansell  
Rensselaer Polytechnic Institute  
Dept. of Metallurgical Engineering  
Troy, NY 12181

Professor J. B. Cohen  
Northwestern University  
Dept. of Material Sciences  
Evanston, IL 60201

Professor M. Cohen  
Massachusetts Institute of Technology  
Department of Metallurgy  
Cambridge, MA 02139

Professor J. W. Morris, Jr.  
University of California  
College of Engineering  
Berkeley, CA 94720

Professor O. D. Sherby  
Stanford University  
Materials Sciences Division  
Stanford, CA 94300

Dr. E. A. Starke, Jr.  
Georgia Institute of Technology  
School of Chemical Engineering  
Atlanta, GA 30332

Professor David Turnbull  
Harvard University  
Division of Engineering and  
Applied Physics  
Cambridge, MA 02139

Dr. D. P. H. Hasselman  
Montana Energy and MHD Research  
and Development Institute  
P.O. Box 3809  
Butte, MT 59701

Dr. L. Hench  
University of Florida  
Ceramics Division  
Gainesville, FL 32601

Dr. J. Ritter  
University of Massachusetts  
Department of Mechanical Engineering  
Amherst, MA 01002

Professor G. Sines  
University of California, Los Angeles  
Los Angeles, CA 90024

Director  
Materials Sciences  
Defense Advanced Research Projects  
Agency  
1400 Wilson Boulevard  
Arlington, VA 22209

Professor H. Conrad  
University of Kentucky  
Materials Department  
Lexington, KY 40506

SUPPLEMENTARY DISTRIBUTION LIST (continued)

Dr. A. G. Evans  
Dept. Material Sciences and  
Engineering  
University of California  
Berkeley, CA 94720

Professor H. Herman  
State University of New York  
Materials Sciences Division  
Stoney Brook, NY 11794

Professor J. P. Hirth  
Ohio State University  
Metallurgical Engineering  
Columbus, OH 43210

Professor R. M. Latanision  
Massachusetts Institute of Technology  
77 Massachusetts Avenue  
Room E-19-702  
Cambridge, MA 02139

Dr. Jeff Perkins  
Naval Postgraduate School  
Monterey, CA 93940

Dr. R. P. Wei  
Lehigh University  
Institute for Fracture and  
Solid Mechanics  
Bethlehem, PA 18015

Professor H. G. F. Wilsdorf  
University of Virginia  
Department of Materials Science  
Charlottesville, VA 22903

Mr. Robert C. Fullerton-Batten  
Kawecki Berylco Industries, Inc.  
P.O. Box 1462  
Reading, PA 19603

Mr. George Keith  
Kawecki Berylco Industries, Inc.  
P.O. Box 1462  
Reading, PA 19603

Mr. Norman Pinto  
Kawecki Berylco Industries, Inc.  
P.O. Box 1462  
Reading, PA 19603

A. G. Gross  
Mechanical Metallurgy Unit  
Autonetics, Inc.  
Anaheim, CA

A. J. Stonehouse  
The Brush Beryllium Co.  
Cleveland, OH

C. W. Marschall  
Columbus Laboratories  
Battelle Memorial Institute  
Columbus, OH

R. E. Maringer  
Columbus Laboratories  
Battelle Memorial Institute  
Columbus, OH